Jilin Daxue Xuebao (Gongxueban)/Journal of Jilin University (Engineering and Technology Edition)
ISSN: 1671-5497
E-Publication: Online Open Access
Vol: 43 Issue: 07-2024
DOI: 10.5281/zenodo.12703134

THE SYNTHESIZATION OF THE Fe_3O_4/GO-ZEOLITE ADSORBENT FOR REMOVING MERCURY FROM WATER SOLUTION

RAMLAN
Department of Physics, Faculty of Natural Sciences, Sriwijaya University, Inderalaya, Ogan Ilir (OI), South Sumatera, Indonesia. Email: ramlan@unsri.ac.id

ENDAH PUSPITA
Department of Physics, Faculty of Natural Sciences, Sriwijaya University, Inderalaya, Ogan Ilir (OI), South Sumatera, Indonesia. Email: endahpuspita1908@gmail.com

AKMAL JOHAN
Department of Physics, Faculty of Natural Sciences, Sriwijaya University, Inderalaya, Ogan Ilir (OI), South Sumatera, Indonesia. Email: akmal_johan@mipa.unsri.ac.id

AKHMAD AMINUDDIN BAMA
Department of Physics, Faculty of Natural Sciences, Sriwijaya University, Inderalaya, Ogan Ilir (OI), South Sumatera, Indonesia. Email: akhmadaminuddin@mipa.unsri.ac.id

MARZUKI NAIBAHO
Physics Department, Faculty of Mathematics and Natural Science, Universitas Indonesia, Depok, Indonesia. Email: sinaibahomarzuki@gmail.com

BUDHY KURNIAWAN
Physics Department, Faculty of Mathematics and Natural Science, Universitas Indonesia, Depok, Indonesia. Email: budhy.kurniawan@sci.ui.ac.id

JANUAR WIDAKDO
Physics Department, Faculty of Mathematics and Natural Science, Universitas Indonesia, Depok, Indonesia. Email: januar.widakdo@ui.ac.id

MASNO GINTING *
Center for Advanced Materials Research (PRMM), National Research and Innovation Agency (BRIN), South Tangerang, Indonesia. *Corresponding Author Email: masn001@brin.go.id

Abstract

The Fe_3O_4/GO-Zeolite adsorbent synthesis has been completed and employed to remove Mercury(Hg(II)) from the water solution. The Fe_3O_4/GO-Zeolite adsorbent was prepared using the coprecipitation method. The Fe_3O_4/GO-Zeolite adsorbent has a surface area of 249.9 m2/g, and an average pore is 2.37 nm. The type of Hg used is Mercury(II) Chloride (HgCl2) or Hg(II), which was diluted in a water solution. The characterizations used in this study were XRD, SEM-EDX, FTIR, VSM, and BET. The best performance of Fe_3O_4/GO-Zeolite adsorbent to adsorb Hg(II) in a water solution that has been achieved is 99.93% with an adsorption capacity of 6.6621 mg/g from the solution with a pH value of 8, temperature of 300C for 30 minutes.

Keywords: Fe_3O_4/GO-Zeolite, Heavy Metal, Mercury, Adsorbents, Adsorption.

Jilin Daxue Xuebao (Gongxueban)/Journal of Jilin University (Engineering and Technology Edition)
ISSN: 1671-5497
E-Publication: Online Open Access
Vol: 43 Issue: 07-2024
DOI: 10.5281/zenodo.12703134

1. INTRODUCTION

The public has always been concerned about environmental degradation, especially water pollution. Mercury (Hg(II)) is among the most dangerous environmental elements. Therefore, it is imperative to eliminate Mercury (Hg(II)) from wastewater before its discharge into the environment.

Mercury (Hg(II)) can be found in the biosphere and aquatic systems. In general, Mercury derived from industries such as the coal industry exists in various forms, including elemental (Hg°), monovalent mercury (Hg(II)), divalent mercury (Hg(II)), and monomethyl mercury ((CH3)Hg) This Mercury penetrates the circulation after being absorbed into the human body, causes various neurological problems, and threatens human health [1], [2].

Hence, removing waste from aquatic systems is essential [3]. Different methods have been developed to treat water pollution from heavy metals, especially Mercury, such as adsorption, oxidation, filtration, precipitation, electrochemical treatment, ion exchange, membrane separation, photochemistry, and irradiation methods[4]–[6].

Adsorption stands out as the premier method for wastewater treatment, boasting numerous advantages, including high removal efficiency, affordability, and absence of contamination [7]. Adsorption generally occurs at solid-liquid interfaces where a substance penetrates the solid or liquid to form a solution. Several conventional adsorbents that can overcome Mercury are silica, activated carbon, Zeolite, graphene oxide, modified chitosan, red mud, mesoporous molecular sieves, composites, and metal oxides[8]–[11].

Unfortunately, their weak adsorbent properties have increased the treatment cost. Among them, magnetic nanoparticles (Fe_3O_4) are emerging as an easy and economical method for absorbent due to their high adsorption capacities and magnetic recoverability.

Fe_3O_4 is a magnetic material that can be used as an adsorbent for Hg in water because it has a high surface area that can produce a high adsorption capacity. The advantage of using Fe_3O_4 as an adsorbent is that it is cheap and non-toxic. However, Fe_3O_4 often undergoes rapid oxidation and easily agglomerates, so additional material is needed to minimize this problem [12]. Graphene oxide (GO) is a material of interest for its large application area.

The combination of magnetic nanoparticles with promising will enhance its properties. GO has a small particle size, large specific surface area, and magnetic solid dipole interactions between Fe_3O_4 nanoparticles. It has chemical stability and high removal performance in water-adsorbing Mercury (Hg(II)) [13]. Research on the removal of Mercury (Hg(II)) using the Fe_3O_4/GO adsorbent was carried out by Bulin et al. (2020), where the adsorption of Mercury (Hg(II)) lasted 4 minutes with an adsorption percentage of 91.17 % [14].

The adsorption percentage and quantity for removing Mercury (Hg(II)) from the aqueous solution were relatively low. To boost the effectiveness of the adsorption process on the Fe_3O_4/GO adsorbent, it is advisable to integrate materials with high ion exchange

Jilin Daxue Xuebao (Gongxueban)/Journal of Jilin University (Engineering and Technology Edition)
ISSN: 1671-5497
E-Publication: Online Open Access
Vol: 43 Issue: 07-2024
DOI: 10.5281/zenodo.12703134

properties, such as Zeolite. As a type of aluminosilicate, natural Zeolite comprises numerous inorganic minerals capable of absorbing heavy metals. Consequently, adding natural Zeolite can enhance the reaction and diminish pollution emissions, including Mercury (Hg(II))[15]. In this study, the Fe_3O_4 adsorbent was synthesized through the coprecipitation method.

Additionally, GO-zeolite was incorporated into the Fe_3O_4 nanoparticles. These materials were utilized to fabricate adsorbents for treating water-containing Mercury (Hg(II)) waste. The Fe_3O_4/GO-Zeolite composite was characterized using XRD, FTIR, SEM-EDS, BET, VSM, and AAS. The notable findings of this research lie in the remarkable potential of these magnetic nanoparticles for adsorbing heavy metal cations, even at deficient concentrations, and their reproducibility.

2. EXPERIMENTAL PROCEDURE

The materials used in this study were 200 mesh commercial iron sand, 32% HCl (Merck), 25% NH_4OH (Technical), Zeolite Clinoptilolite from PT Sari Mas in Medan Indonesia, Graphene Oxide (GO), Ethanol 96% (Technical), NaOH 98% (Technical), and $HgCl_2$ 99% purity Pro Analysis (PA).

As much as 1.5 grams of GO was sonicated for 1 hour. After that, the GO solution was placed on a hot plate, and 1.5 grams of Zeolite was added and stirred for 30 minutes. Add $FeCl_3$ and $FeCl_2$ filtrate from iron sand slowly into the solution and stir at 85^{o}C for 30 minutes. Drop 25% NH_4OH to pH ten and stir for 1 hour.

Precipitate and then wash the residue using filter paper and distilled water. Dry the precipitate using an oven at 60^{o}C, and composites are formed Fe_3O_4/GO-Zeolite. More details can be seen in Figure 1:

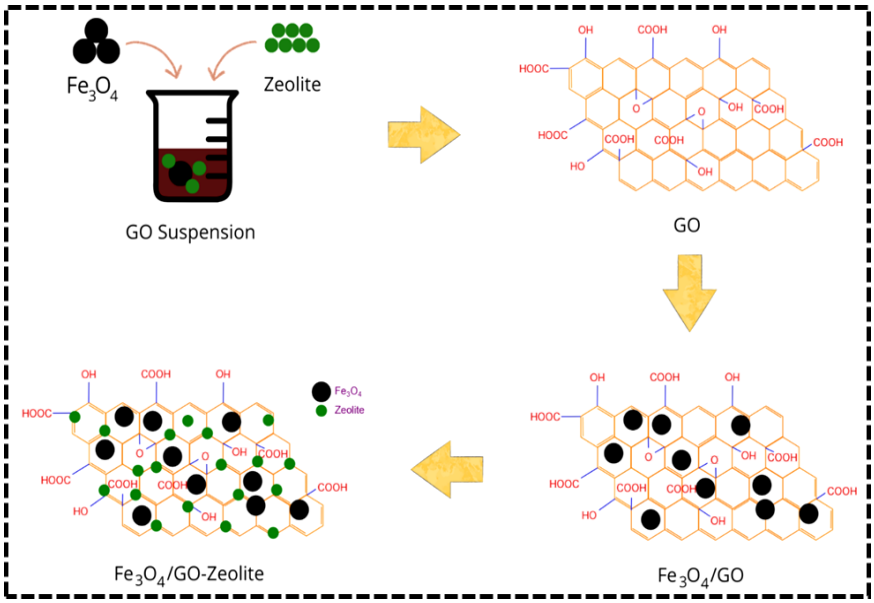

Figure 1: Formation of the chemical structure of the Fe_3O_4/GO-Zeolite adsorbent.

Jilin Daxue Xuebao (Gongxueban)/Journal of Jilin University (Engineering and Technology Edition)
ISSN: 1671-5497
E-Publication: Online Open Access
Vol: 43 Issue: 07-2024
DOI: 10.5281/zenodo.12703134

The techniques utilized in this study encompassed X-Ray Diffraction (XRD; PANalytical AERIS), Scanning Electron Microscope-Energy Dispersive X-Ray (SEM-EDX; PhenomProX Desktop), Fourier-transform infrared spectroscopy (FTIR; Thermo scientific Nicolet iS-10), Vibrating Sample Magnetometer (VSM; VSM250), Brunauer-Emmett-Teller (BET; Surface Area and Pore Size Analyzer Quantachrome Nova 4200e).

Additionally, the performance of Fe_3O_4/GO-Zeolite in the adsorption of Mercury (Hg(II)) was evaluated, considering factors such as pH, contact time, dose, concentration, and temperature.

There is a batch adsorption process. As much as 100 mg of $HgCl_2$ is dissolved in 1 L of distilled water and stirred for 30 minutes. A total of 20 mL of $HgCl_2$ solution was prepared with a pH of 4-8, which was adjusted with HCl 0.1 mol and NaOH 0.1 mol to include 300 mg of Fe_3O_4/GO-Zeolite adsorbent each. Carry out the adsorption process using a shaker for 10 minutes. After that, filter the results of the adsorption process using filter paper, then take the filtrate to characterize CV-AAS.

The adsorption process was carried out with several parameters: pH, contact time, dose, concentration, and temperature. Variations in pH used in the adsorption process started from pH 4, 5, 6, 7, and 8. Variations in contact time used were 10, 20, and 30 minutes.

Variations in doses used were 100, 200, and 300 mg/L, variations in the concentration used were 100, 300, and 500 mg/L, and the temperature variations used were 15, 30, and 45℃. Furthermore, to determine the percentage value of adsorption Ri (%) and adsorption quantity of Qi (mg/g) can be determined using the equation:

$$R_i = \frac{C_0 - C_i}{C_0} \times 100\% \quad (5)$$

$$Q_i = \frac{(C_0 - C_i)V}{m} \quad (6)$$

where C_o is the initial concentration (mg/L), C_i is the final concentration (mg/L), V is the volume of the adsorbed solution (L), and m is the mass of the adsorbent (g) [16].

3. RESULTS AND DISCUSSION

3.1 Characterization of Material Fe_3O_4/GO-Zeolite

The crystal structure formed on the Fe_3O_4/GO-Zeolite adsorbent has been analyzed using XRD, as shown in Figure 2.

Jilin Daxue Xuebao (Gongxueban)/Journal of Jilin University (Engineering and Technology Edition)
ISSN: 1671-5497
E-Publication: Online Open Access
Vol: 43 Issue: 07-2024
DOI: 10.5281/zenodo.12703134

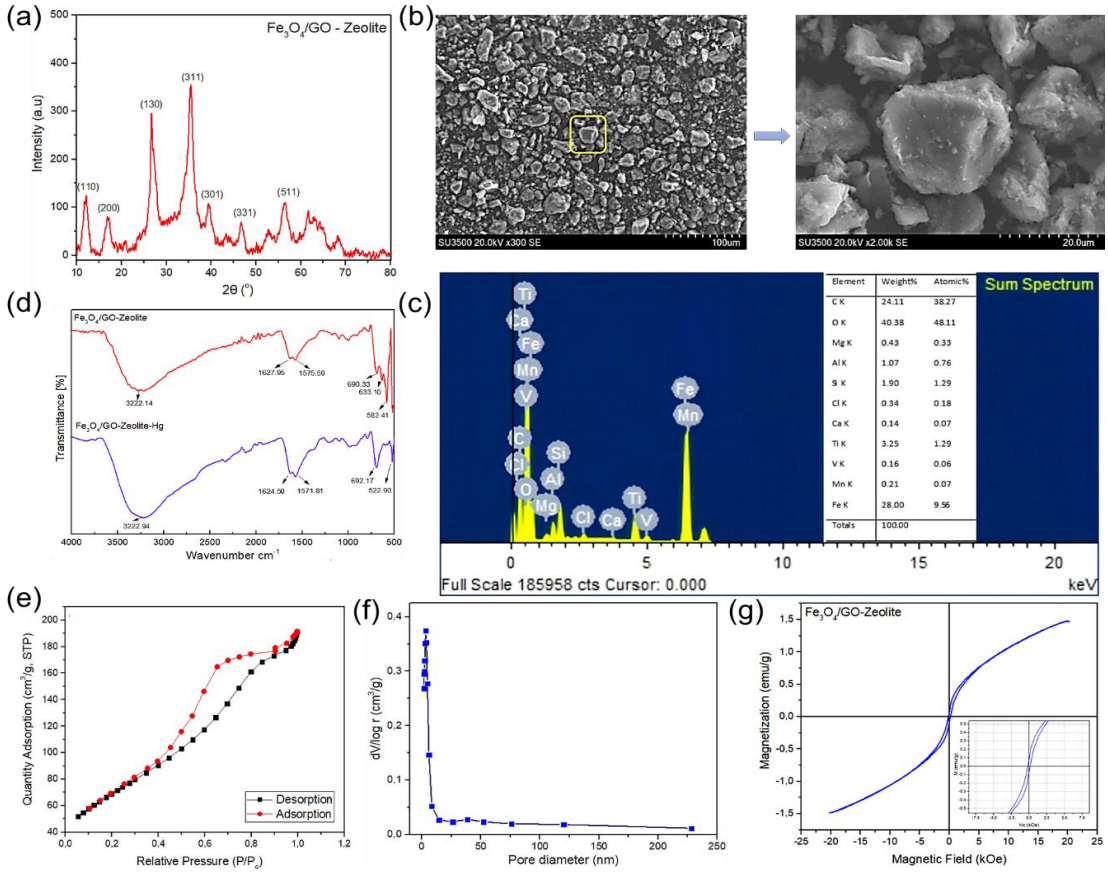

Figure 2: (a) The diffraction pattern, (b) Morphology with 300x and 2000x magnification, (c) Elemental content, (d) IR spectra, (e) BET, (f) BJH, and (g) Hysteresis curve on Fe_3O_4/GO-Zeolite adsorbent.

Based on **Figure 2a**, the diffraction peaks on the Fe_3O_4/GO-Zeolite adsorbent are observed at an angle of 2θ, namely 11.933º, 16.907º, 26.881º, 35.422º, 39.385º, 47.134º, 56.929º with each hkl field (110), (200), (130), (311), (301), (331), (511). The hkl field shows that the Fe_3O_4/GO-Zeolite sample has a positive field direction. In addition, the results from the ICDD database 01-087-2334 confirmed the existence of a magnetite (Fe_3O_4) phase at angles of 35,422º, 47,134º, and 56,929º with a cubic crystal system (fcc). Meanwhile, at angles of 11.933º, 16.907º, 26.881º, 39.385º it indicates that Fe is undergoing oxidation to form a phase of iron oxide (II) hydroxide (FeO(OH)). In addition, GO at peak (110) with 2 θ is 11.933º[17], and Zeolite in the adsorbent was not identified. However, the diffraction peaks with a low intensity that were not identified could be indicated as GO and Zeolite present in the adsorbent.

Figure 2b shows that the Fe_3O_4/GO-Zeolite adsorbent has an irregular grain shape and a rough surface. The rough surface of the adsorbent may be due to the irregularity of GO coating Fe_3O_4 and Zeolite. In addition, the grain size of the adsorbent ranges from 2.5 µm to 42.5 µm. The large size of the adsorbent grains is due to the agglomeration of Fe_3O_4/GO-Zeolite adsorbent particles.

Jilin Daxue Xuebao (Gongxueban)/Journal of Jilin University (Engineering and Technology Edition)
ISSN: 1671-5497
E-Publication: Online Open Access
Vol: 43 Issue: 07-2024
DOI: 10.5281/zenodo.12703134

Furthermore, the EDX results in **Figure 2c** show that the Fe_3O_4/GO-Zeolite adsorbent has several elements: C, O, Mg, Al, Si, Cl, Ca, Ti, V, Mn, and Fe. The highest percentage of elemental content is found in the elements C, O, and Fe, with respective values of 24.11%, 40.38%, and 28.00%. The large percentage of these elements proves that the adsorbent forms Fe_3O_4 and GO compounds. However, Zeolite contains relatively low Al and Si elements, 1.07% and 1.90%, respectively. This indicates that the presence of Zeolite is relatively low in the adsorbent. In addition, the elements Mg, Ca, Ti, V, and Mn are gangue originating from iron sand, while the Cl element probably appeared because of washing GO using HCl.

Figure 2d shows the IR spectra of the Fe_3O_4/GO-Zeolite and Fe_3O_4/GO-Zeolite-Hg adsorbents from wave numbers 4000-500 cm^{-1}. In comparison, the comparison of functional groups at specific wave numbers in the Fe_3O_4/GO-Zeolite and Fe_3O_4/GO-Zeolite-Hg adsorbents is given in Table 1.

Table 1: Functional groups of FTIR on Fe_3O_4/GO-Zeolite and Fe_3O_4/GO-Zeolite-Hg adsorbents.

Adsorbent	Wavenumber (cm^{-1})			
	O-H	C=C	O-Si-O dan O-Al-O	Fe-O
Fe_3O_4/GO-Zeolite	3222.14	1627.95 1575.59	690.33	633.10 582.41
Fe_3O_4/GO-Zeolite-Hg	3222.94	1624.50 1571.81	692.17	522.90

The Fe_3O_4/GO-Zeolite sample displays a broad spectral peak at wave number 3222.14 cm^{-1}, which shows stretching vibrations in the O-H (hydroxyl) groups [23]. The O-H group indicates a hydrogen bond with oxygen, such as the water content in the adsorbent. In addition, the wave numbers 1627.95 cm^{-1} and 1575.59 cm^{-1} show stretching vibrations in the C=C (aromatic) group [24], where the C=C group indicates the presence of carbon elements in the sample.

The emergence of this carbon element can be caused by the vibration of the graphite framework, which does not thoroughly exfoliate during the GO formation process. The 690.33 cm^{-1} shows a symmetrical stretching vibration on the O-Si-O and O-Al-O groups. The O-Si-O and O-Al-O groups indicate a zeolite content bound to oxygen in the adsorbent.

The wave numbers 633.10 cm^{-1} and 582.41 cm^{-1} show high-intensity stretching vibrations in the Fe-O group, associated with vibrational modes in the iron oxide bonds in the Fe_3O_4 crystal lattice [33]. In the Fe_3O_4/GO-Zeolite-Hg sample, several spectra experienced a shift in spectral peaks after adsorption of Hg(II) as in wave number 3222.94 $cm^{-1,}$ which displayed stretching vibrations in the O-H groups.

The O-H group in Fe_3O_4/GO-Zeolite-Hg has a broader spectral peak than Fe_3O_4/GO-Zeolite. This indicates that Fe_3O_4/GO-Zeolite-Hg contains a more significant atomic weight. In the C=C stretching vibration, the peak shifted to lower wave numbers, 1624.50 cm^{-1} and 1571.81 cm^{-1}. However, in the symmetrical stretching vibrations, the O-Si-O and O-Al-O groups experienced a slight shift in peak to a higher wave number of 692.17 cm^{-}

Jilin Daxue Xuebao (Gongxueban)/Journal of Jilin University (Engineering and Technology Edition)
ISSN: 1671-5497
E-Publication: Online Open Access
Vol: 43 Issue: 07-2024
DOI: 10.5281/zenodo.12703134

[1]. In contrast, in the stretching vibrations of Fe-O, the intensity decreased after adsorption on Hg(II), namely at wave number 522.90 cm^{-1}. The presence of the Fe-O group implies that Fe_3O_4 participates in Hg(II) uptake.

It can be seen from **Figure 2e** that there is a red line that shows the amount of reabsorbed nitrogen gas, while the black line indicates the volume of adsorbate gas that is adsorbed at various P/P_o. The surface area contained in the Fe_3O_4/GO-Zeolite adsorbent is 249.9 m^2/g at P/P_o = 0.996883.

Figure 2f shows the size of the adsorption pores on the Fe_3O_4/GO-Zeolite adsorbent, which is 1.69 nm. In addition, the Fe_3O_4/GO-Zeolite adsorbent has an average pore radius of 2.37 nm and an adsorption pore size volume of 0.206 cc/g. The Fe_3O_4/GO-Zeolite adsorbent sample shows a type V isotherm curve with an H2 hysteresis loop [21].

Type V isotherm indicates that the sample is mesoporous, where the adsorbent material has 2 to 50 nm pores. At the same time, the H2 hysteresis loop shows that the distribution and pore size state are not well defined, so the hysteresis loop curve forms a narrow neck with sufficient space size. Broad [22].

Figure 2g shows the shape of the hysteresis curve on the Fe_3O_4/GO-Zeolite adsorbent, where the curve displays a narrow area. This indicates that the Fe_3O_4/GO-Zeolite adsorbent is classified as a soft magnet. In addition, the values of magnetic remanence (Mr) and coercivity (Hc) were 0.07 emu/g and 165.07 Oe, respectively. The results of Mr and Hc show that the magnetic properties of the adsorbent are deficient. This indicates that the adsorbent is superparamagnetic[27].

The low magnetic properties of the adsorbent can be caused by the presence of non-magnetic fractions in the adsorbents, such as GO and Zeolite, which causes shallow saturation magnetization values. The higher the non-magnetic fraction in the adsorbent, the lower the magnetization is [20]. With these magnetic characteristics, the Fe_3O_4 has been composited with GO and Zeolite to reduce the magnetic properties of the adsorbent.

3.2 Performance of Fe_3O_4/GO-Zeolite in the Adsorption of Hg (II)

The effect of pH plays an essential role in the Fe_3O_4/GO-Zeolite adsorbent's carrying out the Hg(II) adsorption process, as well as the adsorption efficiency and adsorption capacity of the adsorption charge. The effect of pH was evaluated at pH 4, 5, 6, 7, and 8, as shown in Figure 3a. Both adsorption efficiency and capacity increase by increasing the pH and tend to saturate above pH at eight values.

Jilin Daxue Xuebao (Gongxueban)/Journal of Jilin University (Engineering and Technology Edition)
ISSN: 1671-5497
E-Publication: Online Open Access
Vol: 43 Issue: 07-2024
DOI: 10.5281/zenodo.12703134

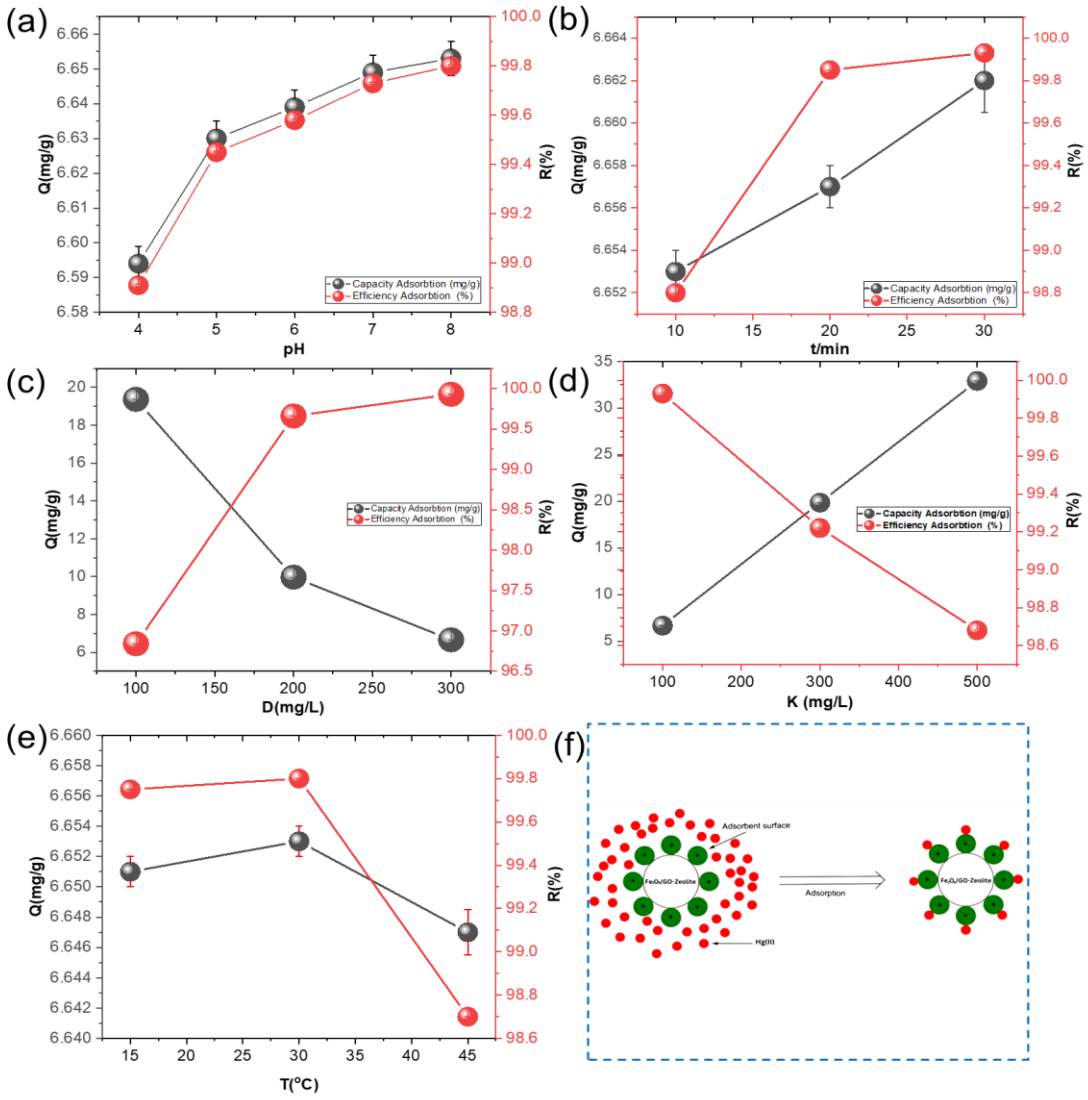

Figure 3: a. Effect of pH (D = 300 mg/L, K = 100 mg/L, and t = 10 minutes), b. The Effect of contact time (D = 300 mg/L, K = 100 mg/L, and pH = 8), c. Effect of adsorbent dose (K = 100 mg/L, t = 30 minutes, and pH = 8) of the Fe_3O_4/GO-Zeolite adsorbent, d. Effect of the concentration of Hg (II) (the Fe_3O_4/GO-Zeolite adsorbent: D = 300 mg/L, t = 30 minutes, and pH = 8), e. Effect of temperature on Hg (II) adsorption using Fe_3O_4/GO-Zeolite adsorbent (D = 300 mg/L, K = 100 mg/L, t = 30 minutes, and pH = 8), f. An Illustration of the adsorption process on Fe_3O_4/GO-Zeolite adsorbent on Hg(II) adsorbate.

During the Hg(II) adsorption process, there has been an increase in adsorption efficiency and adsorption quantity as the pH increases. The pH value of four showed that the Hg(II) solution was acidic, and the adsorption efficiency (98.91%) and quantity (6.5943 mg/g) achieved were low enough. At low pH (less than 4), it seems to be that the H^+ ions prevent

Jilin Daxue Xuebao (Gongxueban)/Journal of Jilin University (Engineering and Technology Edition)
ISSN: 1671-5497
E-Publication: Online Open Access
Vol: 43 Issue: 07-2024
DOI: 10.5281/zenodo.12703134

interaction between the adsorbate and the active adsorbent group so that electrostatic repulsion will occur between Hg (II) and Fe_3O_4/GO-Zeolite, which also has a positive charge. At pH values from 4 to 8, the electrostatic repulsion begins to weaken as the H^+ ions tend to decrease, so the adsorption of Hg(II) increases [35]. The highest adsorption value occurred at a pH of 8, with the adsorption efficiency and adsorption quantity of 99.80% and 6.6534 mg/g, respectively.

The investigation into contact time was conducted at a pH value of 8, with variations in contact time set at intervals of 10, 20, and 30 minutes. The influence of contact time on Hg(II) adsorption is depicted in Figure 3b. Figure 6b shows that at 10 minutes, the adsorption efficiency and quantity are 99.80 % and 6.6534 mg/g. At 20 and 30 minutes, the efficiency and adsorption capacity increased to 99.85% and 6.6569 mg/g. This is probably because an equilibrium had not been reached (Figure 3b), where the Fe_3O_4/GO-Zeolite adsorbent still had an active site side that had not bound the adsorbate, so the adsorption process was still not maximized. As seen at 30 minutes, the adsorption efficiency and quantity produced are 99.93% and 6.6621 mg/g.

The effect of the Fe_3O_4/GO-Zeolite adsorbent doses on the Hg(II) adsorption process was carried out at a pH value of 8 and 30 minutes contact time. The adsorbent doses used for this adsorption were 100, 200, and 300 mg/L adsorbent, which is given in Figure 3c. Using Fe_3O_4/GO-Zeolite doses of 100, 200, and 300 mg/L resulted in an adsorption percentage of 96.84, 99.66, and 99.93%, while the adsorption quantity decreased by 19.3693 mg/g, 9.9669 mg/g, and 6.6621 mg/g. The high amount of adsorbent can certainly absorb more Hg(II).

The adsorption sites are also increasing so that they can bind more adsorbate. However, high doses of absorbent can also reduce adsorption capacity. This is due to disturbances such as clumping on the adsorbent so that some surface parts are not entirely exposed, and the absorption process becomes ineffective. In addition, the increase in adsorption capacity on the adsorbate is inversely proportional to the amount of adsorbent, where the adsorption capacity functions to measure the metal ions adsorbed on each unit weight of the adsorbent.

The effect of concentration on the adsorption process was carried out at a pH of 8, 300 mg/L adsorbent dose, and a contact time of 30 minutes. The Hg(II) adsorbate concentration used in adsorption was 100, 300, and 500 mg/L. The effect of the adsorbate concentration, Hg (II), on the Fe_3O_4/GO-Zeolite adsorbent is given in Figure 3d. At adsorbate concentration levels of 100, 300, and 500 mg/L, the adsorption efficiency values decreased to 99.93%, 99.22%, and 98.68%, respectively, while the corresponding adsorption capacity values increased to 6.6621, 19.8459, and 32.8953 mg/g, respectively.

The decrease in the adsorption efficiency value could be due to the Fe_3O_4/GO-Zeolite adsorbent being unable to absorb all of the Hg(II) concentration, which was too high compared to the adsorbent dose. In addition, using a high level of adsorbate concentration results in a high adsorption capacity. This could be due to the increasing number of Hg(II) ions in the solution. The more Hg(II) ions adsorbed into the active site

Jilin Daxue Xuebao (Gongxueban)/Journal of Jilin University (Engineering and Technology Edition)
ISSN: 1671-5497
E-Publication: Online Open Access
Vol: 43 Issue: 07-2024
DOI: 10.5281/zenodo.12703134

on the Fe_3O_4/GO-Zeolite adsorbent's surface, the greater the adsorption capacity. If the concentration level of Hg(II) ions is higher than the amount of Fe3O4/GO-Zeolite adsorbent, the availability of active sites for Fe_3O_4/GO-Zeolite adsorbents decreases and will not be able to absorb all Hg(II) ions.

The impact of temperature on the adsorption process was investigated under pH 8 conditions, with 300 mg/L of adsorbent doses and 100 mg/L of adsorbate concentration over 30 minutes. The temperature variations used in the adsorption process were 15, 30, and 45ºC. The effect of temperature on the adoption of Hg(II) using Fe_3O_4/GO-Zeolite adsorbent is given in Figure 3e. From 30℃ to 45℃, the adsorption efficiency and capacity both decrease. This could be caused by temperatures that are too high, which can cause desorption between the adsorbent and the adsorbent. In addition, higher temperatures cause the movement of Hg(II) ions to be faster, so Hg(II) ions are more challenging to adsorb by the Fe_3O_4/GO-Zeolite adsorbent. Therefore, 30℃ is the optimum temperature for absorbing Hg(II) in solution.

4. CONCLUSION

This research has successfully synthesized the adsorbent Fe_3O_4/GO-Zeolite and used it to remove Mercury (Hg (II)) from the water solution. From the XRD results, the sample showed the presence of the Fe_3O_4 phase, while the GO and zeolite phases were not identified. However, the presence of the GO and Zeolite phases was detected from the results of the IR spectrum. The SEM results showed that the shape of the Fe_3O_4/GO-Zeolite adsorbent particles was irregular, with a rough surface caused by the irregularity of GO in coating Fe_3O_4 and Zeolite.
VSM measurement found that the Fe_3O_4/GO-Zeolite adsorbent exhibits relatively low magnetic properties due to many non-magnetic fractions, such as GO and Zeolite, which causes shallow saturation magnetization values. In the adsorption process of Mercury (Hg (II)) in water solution, the Fe_3O_4/GO-Zeolite adsorbent has been successful in absorbing Hg (II) with the optimum percentage and adsorption capacity of 99.93% and 6.662 mg/g for 30 minutes where the Fe_3O_4/GO-adsorbent Zeolite has a surface area and an average pore size of 249.9 m^2/g and 2.37 nm, respectively.

Acknowledgment

This article's research and publication were the result of collaboration between the National Research and Innovation Agency (BRIN) and Universitas Sriwijaya, with partial funding provided by DIPA of the Public Service Agency of Universitas Sriwijaya in 2023, under Reference Number SP DIPA-023.17.2.677515/2023, dated November 30, 2022. Additionally, this collaboration was authorized by Rector's Decree Number: 0188/UN9.3.1/SK/2023, issued on April 18, 2023.

Credit authorship contribution statement

Ramlan: Conceptualization, Project administration, Writing - original draft, review & editing. **Marzuki Naibaho**: Methodology, Investigation, Data Curation & Resources. **Budhy Kurniawan**: Formal analysis, Writing review & editing. **Januar Widakdo**: Investigation, Formal analysis, **Endah Puspita**: Methodology, Investigation, Formal analysis. **Akmal Johan**: Investigation. **Akhmad Aminuddin Bama**: Formal analysis. **Masno Ginting**: Supervision, and write - review & editing.

Jilin Daxue Xuebao (Gongxueban)/Journal of Jilin University (Engineering and Technology Edition)
ISSN: 1671-5497
E-Publication: Online Open Access
Vol: 43 Issue: 07-2024
DOI: 10.5281/zenodo.12703134

References

1) J. Tang *et al.*, “Mercury adsorption kinetics on sulfurized biochar and solid-phase digestion using aqua regia: A synchrotron-based study,” *Chem. Eng. J.*, vol. 428, no. July 2021, p. 131362, 2022, doi: 10.1016/j.cej.2021.131362.

2) S. Mitra *et al.*, “Impact of heavy metals on the environment and human health: Novel therapeutic insights to counter the toxicity,” *J. King Saud Univ. - Sci.*, vol. 34, no. 3, p. 101865, 2022, doi: 10.1016/j.jksus.2022.101865.

3) K. Parajuli, A. K. Sah, and H. Paudyal, “Green Synthesis of Magnetite Nanoparticles Using Aqueous Leaves Extracts of <i>Azadirachta indica</i> and Its Application for the Removal of As(V) from Water,” *Green Sustain. Chem.*, vol. 10, no. 04, pp. 117–132, 2020, doi: 10.4236/gsc.2020.104009.

4) J. Du, B. Zhang, J. Li, and B. Lai, “Decontamination of heavy metal complexes by advanced oxidation processes: A review,” *Chinese Chem. Lett.*, vol. 31, no. 10, pp. 2575–2582, 2020, doi: 10.1016/j.cclet.2020.07.050.

5) W. S. Chai *et al.*, “A review on conventional and novel materials towards heavy metal adsorption in wastewater treatment application,” *J. Clean. Prod.*, vol. 296, p. 126589, 2021, doi: 10.1016/j.jclepro.2021.126589.

6) Q. Chen, Y. Yao, X. Li, J. Lu, J. Zhou, and Z. Huang, “Comparison of heavy metal removals from aqueous solutions by chemical precipitation and characteristics of precipitates,” *J. Water Process Eng.*, vol. 26, no. October, pp. 289–300, 2018, doi: 10.1016/j.jwpe.2018.11.003.

7) J. Liu *et al.*, “Rapid removal of Cr(III) from high-salinity wastewater by cellulose-g-poly-(acrylamide-co-sulfonic acid) polymeric bio-adsorbent,” *Carbohydr. Polym.*, vol. 270, no. 2, 2021, doi: 10.1016/j.carbpol.2021.118356.

8) R. Foroutan, S. J. Peighambardoust, A. Ahmadi, A. Akbari, S. Farjadfard, and B. Ramavandi, “Adsorption mercury, cobalt, and nickel with a reclaimable and magnetic composite of hydroxyapatite/Fe_3O_4/polydopamine,” *J. Environ. Chem. Eng.*, vol. 9, no. 4, p. 105709, 2021, doi: 10.1016/j.jece.2021.105709.

9) A. H. Jawad, A. S. Abdulhameed, A. Reghioua, and Z. M. Yaseen, “Zwitterion composite chitosan-epichlorohydrin/zeolite for adsorption of methylene blue and reactive red 120 dyes,” *Int. J. Biol. Macromol.*, vol. 163, pp. 756–765, 2020, doi: 10.1016/j.ijbiomac.2020.07.014.

10) W. Qu, T. Yuan, G. Yin, S. Xu, Q. Zhang, and H. Su, “Effect of properties of activated carbon on malachite green adsorption,” *Fuel*, vol. 249, no. October 2018, pp. 45–53, 2019, doi: 10.1016/j.fuel.2019.03.058.

11) B. N. Mahato, T. Krithiga, and M. A. Mary Thangam, “Rapid adsorption of As(V) from aqueous solution by ZnO embedded in mesoporous aluminosilicate nanocomposite adsorbent: Parameter optimization, kinetic, and isotherms studies,” *Surfaces and Interfaces*, vol. 23, no. V, p. 100636, 2021, doi: 10.1016/j.surfin.2020.100636.

12) R. Cao, M. Fan, J. Hu, W. Ruan, K. Xiong, and X. Wei, “Optimizing low-concentration mercury removal from aqueous solutions by reduced graphene oxide-supported Fe_3O_4 composites with the aid of an artificial neural network and genetic algorithm,” *Materials (Basel).*, vol. 10, no. 11, 2017, doi: 10.3390/ma10111279.

13) T. Guo *et al.*, “Efficient removal of aqueous Pb(II) using partially reduced graphene oxide-Fe_3O_4,” *Adsorpt. Sci. Technol.*, vol. 36, no. 3–4, pp. 1031–1048, 2018, doi: 10.1177/0263617417744402.

14) C. Bulin, B. Li, Y. Zhang, and B. Zhang, “Removal performance and mechanism of Fe_3O_4/graphene oxide as an efficient and recyclable adsorbent toward aqueous Hg(II),” *Res. Chem. Intermed.*, vol. 46, no. 10, pp. 4509–4527, 2020, doi: 10.1007/s11164-020-04217-5.

Jilin Daxue Xuebao (Gongxueban)/Journal of Jilin University (Engineering and Technology Edition)
ISSN: 1671-5497
E-Publication: Online Open Access
Vol: 43 Issue: 07-2024
DOI: 10.5281/zenodo.12703134

15) L. Ma *et al.*, “Reducing CO/NO and absorbing heavy metals in self-sustained smouldering of high-moisture sludge by regulating inert media with low-cost natural zeolite,” *Environ. Pollut.*, vol. 337, no. September, p. 122556, 2023, doi: 10.1016/j.envpol.2023.122556.

16) J. Ndi Nsami and J. Ketcha Mbadcam, “The adsorption efficiency of chemically prepared activated carbon from cola nut shells by ZnCl2 on methylene blue,” *J. Chem.*, vol. 2013, 2013, doi: 10.1155/2013/469170.

17) P. A. Mikhaylov, M. I. Vinogradov, I. S. Levin, G. A. Shandryuk, A. V. Lubenchenko, and V. G. Kulichikhin, “Synthesis and characterization of polyethylene terephthalate-reduced graphene oxide composites,” *IOP Conf. Ser. Mater. Sci. Eng.*, vol. 693, no. 1, 2019, doi: 10.1088/1757-899X/693/1/012036.

18) L. Guo *et al.*, “A facile route to synthesize magnetic particles within hollow mesoporous spheres and their performance as separable Hg2+ adsorbents,” *J. Mater. Chem.*, vol. 18, no. 23, pp. 2733–2738, 2008, doi: 10.1039/b802857e.

19) G. Li, Z. Zhao, J. Liu, and G. Jiang, “Effective heavy metal removal from aqueous systems by thiol functionalized magnetic mesoporous silica,” *J. Hazard. Mater.*, vol. 192, no. 1, pp. 277–283, 2011, doi: 10.1016/j.jhazmat.2011.05.015.

20) D. Jiao, K. Lesage, M. Y. Yardimci, C. Shi, and G. De Schutter, “Possibilities of fly ash as responsive additive in magneto-rheology control of cementitious materials,” *Constr. Build. Mater.*, vol. 296, p. 123656, 2021, doi: 10.1016/j.conbuildmat.2021.123656.

21) K. K. Yadav, R. Wadhwa, N. Khan, and M. Jha, “Efficient metal-free supercapacitor based on graphene oxide derived from waste rice,” *Curr. Res. Green Sustain. Chem.*, vol. 4, p. 100075, 2021, doi: 10.1016/j.crgsc.2021.100075.

22) Z. A. Alothman, “A review: Fundamental aspects of silicate mesoporous materials,” *Materials (Basel).*, vol. 5, no. 12, pp. 2874–2902, 2012, doi: 10.3390/ma5122874.

23) F. Mouhat, F. X. Coudert, and M. L. Bocquet, “Structure and chemistry of graphene oxide in liquid water from first principles,” *Nat. Commun.*, vol. 11, no. 1, pp. 1–9, 2020, doi: 10.1038/s41467-020-15381-y.

24) J. Wang, M. Sun, C. Chu, J. Yuan, and C. Xing, “Fixation Effect of Fe_3O_4-GO to Hinder Pb(II) Translocation into Leek,” *Water. Air. Soil Pollut.*, vol. 231, no. 7, 2020, doi: 10.1007/s11270-020-04694-9.

25) A. E. da Costa Júnior *et al.*, “A self-assembly of graphene oxide@Fe_3O_4/metallo-phthalocyanine nanohybrid materials: synthesis, characterization, dielectric and thermal properties,” *J. Mater. Sci.*, vol. 52, no. 16, pp. 9546–9557, 2017, doi: 10.1007/s10853-017-1133-3.

26) E. Patrikiadou, A. Patrikidou, E. Hatzidaki, P. Christos N, V. Zaspalis, and L. Nalbandian, “Magnetic Nanoparticles in Medical Diagnostic Applications: Synthesis, Characterization and Proteins Conjugation,” *Curr. Nanosci.*, vol. 12, no. 4, pp. 455–468, 2015, doi: 10.2174/1573413712666151210230002.

27) D. Zhang, G. Crini, E. Lichtfouse, B. Rhimi, and C. Wang, “Removal of Mercury Ions from Aqueous Solutions by Crosslinked Chitosan-based Adsorbents: A Mini Review,” *Chem. Rec.*, vol. 20, no. 10, pp. 1220–1234, 2020, doi: 10.1002/tcr.202000073.